CHAPTER V
EFFECTS OF NON-IONIC AND CATIONIC SURFACTANT ON POROUS STRUCTURE OF POLYBENZOXAZINE-BASED CARBON XEROGELS

5.1 Abstract

Polybenzoxaxine (PBZ), a new type of additional-cure phenolic system, has been successfully synthesized by a facile quasi-solventless method and used as a precursor for producing carbon xerogels. In this work, we aim to study the effect of non-ionic (Synperonic NP30) and cationic (CTAB) surfactants on porous structure of polybenzoxazine-based carbon xerogels. Inter-connected structure of mesoporous carbon xerogels with mesopore diameters in the range of 15.57-36.07 nm was obtained by using different concentrations of CTAB. In addition, carbon xerogel nanospheres with the size of 50-200 nm were also obtained through the emulsion process. The mesopore diameters started to decrease when the carbon xerogel nanospheres were formed at the CTAB concentration of equal to or exceeding 0.030 M. By using Synperonic NP30 as a surfactant, the properties of the obtained carbon xerogels were shifted from mesoporous materials for the reference carbon xerogel (no surfactant added) to obviously microporous materials at higher concentrations of Synperonic NP30 (0.009 M - 0.180 M). The carbon xerogel microspheres with the diameter size of about 2.5 μm were also obtained through the emulsion process when the concentration of Synperonic NP30 was reached at 0.180 M.

5.2 Introduction

Resorcinol(R)-Formaldehyde(F)-based organic gel and its carbon gel after pyrolysis were first introduced by Pekala et al. [1, 2]. Carbon gel could be mainly classified into three type viz. carbon aerogel, carbon cryogel, and carbon xerogel; depending on the drying method during solvent removal process [1-7]. Carbon gel is a porous material which possess various outstanding properties. Some of these properties are: light weight, high surface area, high porosity, high thermal stability, and low density, etc. According to its outstanding properties, carbon gel has been used in many applications such as catalyst supporting material [5, 8, 9], energy storage [10-12], and molecular sieve material for gas separation technology [13, 14], etc.

Nowadays, development of carbon materials is becoming the great topic of research due to the growth of carbon materials consumption in many applications, especially, understanding the effects of parameters on pore size, pore volume, and specific surface area of carbon materials. Of interesting in pore size, generally, the formation of pore in carbon gel could be classified into two type; micropore (<2 nm) located within the carbon particle and meso-macropore (2-50 nm and >50 nm) formed by inter-connection of carbon particles during the phase separation phenomena [1, 2, 15, 16]. Microporosity of carbon gel could be easily managed by many activation processes [16-19]. However, the generation of meso-macroporosity was mainly depended on the behavior of phase separation mechanism between polymer and solvent in the sol-gel process [1-2]. Many new routes to generate meso-macroporosity of carbon gels have been reported for example: surfactant-templated method [20, 21], emulsion method [22, 23], and hard-templated method [24, 25], etc.

Moreover, many materials have been used as precursors for syntheses of carbon gels [1, 2, 26-28], especially, resorcinol-formaldehyde (RF) polymer. However, production of RF has some disadvantages which are: the need of two weeks with multi-steps to complete the process, the need of harsh catalyst for polymerization, limited molecular design flexibility, and releasing by-product during polymerization [1, 2, 29].

In this work, polybenzoxazine (PBZ) was proposed to be used as a candidate material for the production of carbon gel. The exceptional properties of polybenzoxazine that overcome those drawbacks of RF are: high thermal stability, no need of harsh catalyst or initiator for polymerization, no releasing of toxic by-product during polymerization, near zero shrinkage after polymerization, excellent mechanical integrity, high cabonaceous yield, great molecular design flexibility, especially, high crosslink density [30-34]. In particular, the crosslink density was quite important because high crosslink density not only leads to improvement of thermo-oxidative stability enabling high cabonaceous yield after carbonization [34], but also results in the preservation of porosity, especially, mesoporosity, after the solvent removal process.

PBZ is a cross-linked polymer with additional extensive hydrogen bonded networks which can withstand pore collapse without the need of supercritical CO_2 drying process. The shorter preparation time with fewer synthesis steps is required when PBZ is used as a precursor for carbon xerogels preparation.

PBZ was generally synthesized by the Manich polycondensation reaction of phenol, formaldehyde, and amine, via a quasi-solventless route adapted from the solventless method, proposed by Ishida [39]. In 2009, PBZ-based carbon aerogels were first introduced by Lorjai et al. who found that their carbon aerogel exhibited the properties as a microporous material [35]. In 2010, PBZ-based carbon aerogels with an average pore diameter of 3.67 nm were used as an electrode in supercapacitors by Katanyoota et al. [36]. As mentioned above, it was found that PBZ-based carbon shows the pore diameter in a range of small micro-mesopore. This property could affect the utilization of polybenzoxazine-based carbon for various applications that needed large pore diameter.

For application as the catalyst supporting material, those small pore sizes of PBZ-based carbon aerogels might limit the catalytic efficiency for reactions that are involved with large molecules due to the limitation of mass transfer of large molecules [37-38].

In this work, we aim to study the effect of cationic and non-ionic surfactant on porous structure of PBZ-based carbon xerogels, in order to improve the pore

diameter. The textural characteristic of the obtained carbon xerogels were also be investigated.

5.3 Experimental

5.3.1 Materials

Main-chain type benzoxazine polymer (abbreviated as MCBP) with benzoxazine group as a part of the chemical repeat unit was synthesized by the Manich polycondensation reaction of bisphenol-A (BA, 97%, Aldrich), formaldehyde (37%, Merck Limited, Germany), and triethylenetetramine (TETA, 85%, Facai Group Limited, Thailand) using dioxane (analytical grade, Labscan Asia Co., Ltd., Thailand) as a solvent. Non-ionic surfactant, Synperonic NP30 (Polyethylene glycol nonylphenyl ether, >99.8%), and cationic surfactant, Hexadecyltrimethylammonium bromide [$CH_3(CH_2)_{15}N(Br)(CH_3)_3$, CTAB, >99.8%], were purchased from Fluka. Ethyl alcohol (>98%) was purchased from J.T. Baker. All chemical were used without further purification.

5.3.2 Synthesis of polybenzoxazine-based carbon xerogels (PBZ-based carbon xerogels)

MCBP was synthesized by a quasi-solventless method adopted from the solventless method proposed by Ishida et al. [39]. The molar ratio of reactant was 1:1:4 in which belong to BA, TETA, and formaldehyde, respectively. MCBP derived from bisphenol-A and TETA was hereinafter abbreviated as MCBP(BA-teta). The solid content of MCBP(BA-teta) was fixed at 10% w/w. BA was dissolved in dioxane and magnetically stirred for 20 minutes. Then, surfactant was mixed and stirred for 30 minutes. Afterwards, formaldehyde was then added and continuously stirred for 20 minutes. Finally, TETA was slowly dropped into the mixture and continuously stirred for 1 h until the transparent yellow pale solution was obtained. Unlike the conventional method which took 5h, the reaction was completed within an hour [33]. The MCBP(BA-teta) solution was sealed off in a glass vial and left for 24

h. The MCBP(BA-teta) solution was further heated in an oil bath at 80 °C for 2 days to form the white-opaque-MCBP(BA-teta) organogel. The MCBP(BA-teta) organogel was taken out from glass vial and cut into a cubic shape. Soxhlet technique was used to remove all residual surfactant and solvent in the organogel by using ethyl alcohol as a carrier phase under heating temperature of 100 °C for 24 h and reflux temperature of 10 °C. After that, the MCBP(BA-teta) organogel was heated at 90 °C for 24 h to remove all residual ethanol. The MCBP(BA-teta) organogel was placed in an oven for step-curing at 160 °C and 180 °C for 3 h at each temperature, and 200 °C for 1 h to achieve the fully-cured polybenzoxazine xerogel [36, 40]. After step-curing, fully-cured polybenzoxazine xerogel was carbonized under nitrogen flow of 600 cm^3/min using the following cycle step: 30–250 °C for 1 h, 250–600 °C for 5 h, 600–800 °C for 1 h and hold at 800 °C for 2 h, and then an oven was cooled to room temperature under nitrogen atmosphere [36, 40].

Polybenzoxazine-based carbon xerogels derived from Synperonic NP30 and CTAB as surfactants during synthesis of MCBP(BA-teta) solution were denoted as CX-NP30-xx and CX-CTAB-xx where NP30 and CTAB were nomenclatures of Synperonic NP30 (Polyethylene glycol nonylphenyl ether) and CTAB (Hexadecyltrimethylammonium bromide) by evaporation drying (CX=Carbon xerogel), respectively. The numbers represented in the nomenclatures (-xx) show different concentrations of surfactants in molar unit.

5.3.3 Identification of microstructure and morphology of polybenzoxazine-based carbon xerogels

Morphology and microstructure of carbon xerogels were observed by field emission scanning electron microscope (FE-SEM, Hitachi/S-4800 model) and transmission electron microscope (TEM, JEOL 2010F). Quantachrome-Autosorp1-MP was used to determine the porous structure of the samples. Approximately 0.1 g of carbon xerogels were degassed at 250 °C for 15 h to remove all the adsorbed species. The specific surface area (S_{BET}) was calculated by BET algorithm (Brunauer-Emmett-Teller) [41]. Micropore volume (V_{mic}) was analyzed by t-plot

method [42]. Micropore size distributions were analyzed by MP method (Standard micropore size distribution). Mesopore volume (V_{mes}) and mesopore size distributions were analyzed by BJH (Barrett-Johner-Halendar) algorithm [43, 44].

5.4 Results and Discussion

5.4.1 Effects of Cationic surfactant (Hexadecyltrimethylammonium-bromide, CTAB) on porous structure of PBZ-based carbon xerogels

Polybenzoxazine (PBZ)-based carbon xerogels were synthesized by using CTAB as a surfactant as described in experimental section. The morphologies of the obtained PBZ-based carbon xerogels were observed by FE-SEM technique. Figure 5.1 shows the SEM micrographs of PBZ-based carbon xerogels synthesized at different concentrations of CTAB from 0.003 M to 0.180 M.

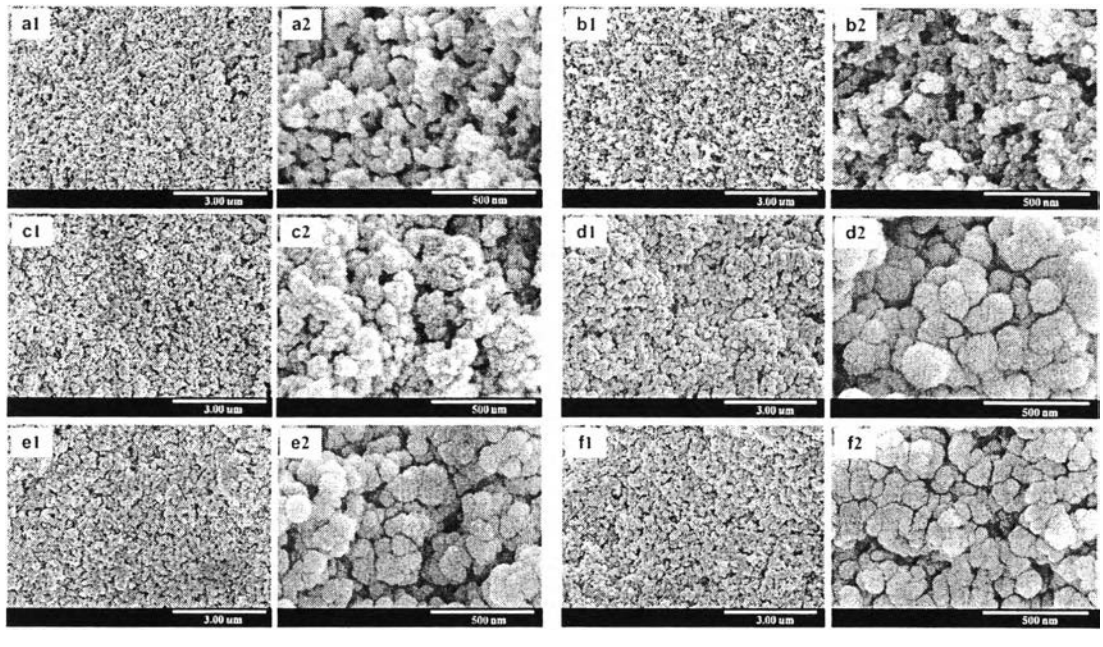

Figure 5.1 SEM micrographs of PBZ-based carbon xerogels prepared from 10% w/w of benzoxazine precursor using different concentrations of CTAB; (a) no added CTAB, (b) 0.003 M, (c) 0.009 M, (d) 0.030 M, (e) 0.090 M, and (f) 0.180 M; 1: low magnification; 2: high magnification.

All samples show the 3D-inter-connected structure formed by carbon nanoparticles. However, Figures 5.1a and b show the 3D-network of carbon nanoparticles with less agglomeration. These carbon nanoparticles are slightly hard to distinguish in sample CX (Figure 5.1a, reference carbon xerogel) and sample CX-CTAB-0.003 (Figure 5.1b). After increasing the concentration of CTAB to 0.009 M, sample CX-CTAB-0.009 not only shows the 3D-network of carbon nanoparticles, but also starts to form the small-spherical-like carbon nanoparticles with the size of about 100 nm, as illustrated in Figure 5.1c. When the concentration of CTAB was increased to 0.030 M, 0.090 M, and-0.180 M, the carbon xerogel nanospheres were obtained with the size of about 100-200 nm for CX-CTAB-0.030, 50-100 nm for CX-CTAB-0.090 and CX-CTAB-0.180, respectively, as shown in Figures 5.1d-f. Moreover, Figures 5.1d-f (CX-CTAB-0.030 – CX-CTAB-0.180) also show the dense morphologies comparing to those in Figures 5.1a and b which will be discussed later.

To explain the formation of carbon xerogel nanospheres and the sizes of nanospheres, the micelle formation of CTAB was used to clarify. After dissolution of CTAB into the solvent, CTAB molecules will be dissociated as individual molecule in the solvent. If the concentration of CTAB was equal to the critical micelle concentration (CMC), the molecules of CTAB were then oriented into spherical micelles with hydrophilic head groups toward the solvent and hydrophobic tail groups away from the solvent. In this study, polybenzoxazine [MCBP(BA-teta)] shows the hydrophobic property. Therefore, after micelle formation of CTAB, polybenzoxazine cluster would be then formed at the interior region (inner core) of the micelles and then grow into nanospheres. Illustrated in Figure 5.2a is the formation model of benzoxazine nanospheres formed inside the interior region of CTAB micelle. The similar results were also found by many research groups for resorcinol-formaldehyde polymer [22, 23, 45]. As mentioned earlier, CX-CTAB-0.030, CX-CTAB-0.090, and CX-CTAB-0.180 showed the nanospherical shape which can be implied that the CTAB molecules started to form spherical micelle at 0.030 M. Although the particle shape of CX-CTAB-0.090 and CX-CTAB-0.018 was spherical as same as those of CX-CTAB-0.030, the particle sizes of CX-CTAB-0.090 and CX-CTAB-0.018 were smaller than those of CX-CTAB-0.030. This phenomenon can be explained in the term of the smaller size of micelle formation.

When the concentration of CTAB was exceeded the CMC, the shape of micelle was still in a spherical shape but reduced into smaller sizes depending on packing parameter [46]. However, Figure 5.1f reveals the unclear-deformed carbon xerogel nanospheres which might be due to the deformation of spherical micelle into other structures.

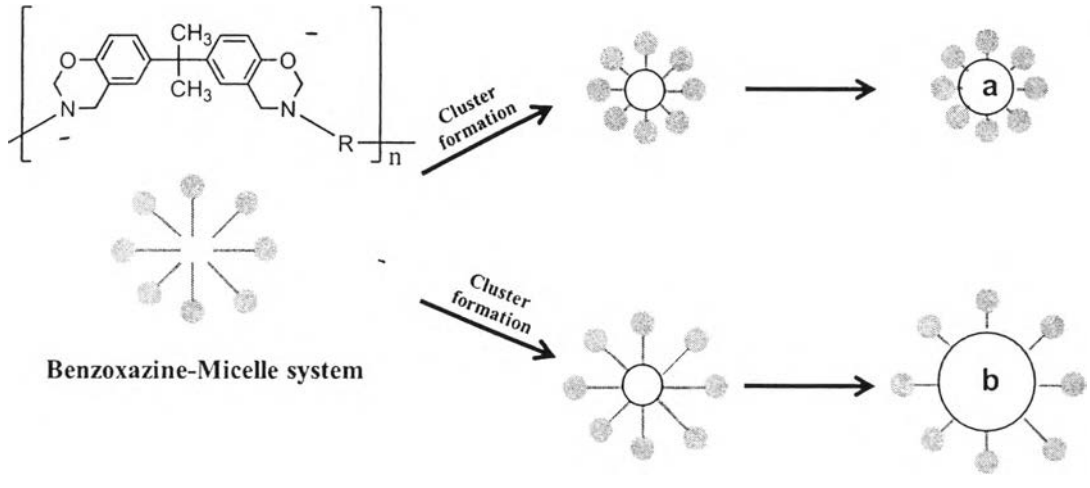

Figure 5.2 Scheme of the benzoxazine-micelle formation; (a) nanospheres for CTAB system, (b) microspheres for Synperonic NP30 system.

The porous structures of PBZ-based carbon xerogels using CTAB as a surfactant were tabulated in Table 5.1. All samples exhibit high amount of mesopore volume with an average mesopore diameter in the range of 15.57-36.07 nm. CX-CTAB-0.090 shows the highest BET surface area of 369 m^2/g with the highest amount of mesopore volume of 0.64 cc/g. The surface area of the samples tend to increase with the decrease of mesopore diameters. The smaller pore diameter could provide large surface area compared to those of larger pore diameter. However, at the concentration of 0.180 M CTAB, the BET surface area of CX-CTAB-0.180 was decreased to 271 m^2/g, even though the mesopore diameter of the sample was about 15.57 nm. This can be described by the dense morphology and the deformation of xerogel network due to the deformation of carbon xerogel nanospheres at high concentration of CTAB.

Table 5.1 Pore structure of PBZ-based carbon xerogels prepared from 10% w/w of benzoxazine precursor using different concentrations of CTAB

Sample	S_{BET} (m^2/g)	V_{micro} (cm^3/g)	V_{meso} (cm^3/g)	V_{total} (cm^3/g)	APD_{micro} (nm)	APD_{meso} (nm)
CX	280	0.08	0.20	0.28	0.76	34.78
CX-CTAB-0.003	284	0.11	0.21	0.32	0.66	35.85
CX-CTAB-0.009	275	0.10	0.19	0.29	0.80	36.07
CX-CTAB-0.030	323	0.12	0.20	0.32	0.76	25.38
CX-CTAB-0.090	369	0.12	0.52	0.64	1.00	25.25
CX-CTAB-0.180	271	0.10	0.17	0.27	0.66	15.57

Notes : S_{BET}: BET surface area; S_{meso}: mesopore surface area; V_{micro}: micropore volume; V_{meso}: mesopore volume; V_{total}: total pore volume; APD_{micro}: average micropore diameter; APD_{meso}: average mesopore diameter; APD: average pore diameter

Interestingly, in this study, wide ranges of mesopore diameter were achieved by changing the concentrations of CTAB. The mesopore diameters were 34.78, 35.85, 36.07, 25.38, 25.25, and 15.57 nm for CX, CX-CTAB-0.003, CX-CTAB-0.009, CX-CTAB-0.030, CX-CTAB-0.090, and CX-CTAB-0.180, respectively. According to the literature proposed by Wang et al. [16], the large mesopore diameter ranging from 5-40 nm was created by inter-connected structure of carbon nanoparticle. Moreover, the micropores ($\leq$ 2 nm) and small mesopores (2-5 nm) were located within the carbon nanoparticles [16]. Therefore, in this study, the mesopore diameters varying from 15.57-36.07 nm should be generated by the inter-connected structure of carbon nanoparticles and very small micropore diameters were located within carbon nanoparticle due to the carbonization process. At low concentrations of CTAB (CX-CTAB-0.003 and CX-CTAB-0.009), the carbon xerogel nanospheres were not formed because those concentrations did not reach the CMC value, resulting in the formation of single CTAB molecules instead. Therefore, the mesopore structure and the carbon nanoparticles generated in these cases could be mainly affected by the sol-gel process due to the phase separation phenomena rather than those generated by inter-connection of carbon xerogel nanospheres produced at the interior region of the micelles. However, the mesopore diameters of

CX-CTAB-0.003 (35.85 nm) and CX-CTAB-0.009(36.07 nm) were slightly larger than that of CX (34.78 nm). This can be described by the electrostatic force between cationic surfactant (CTAB) species and anionic polymer chains of polybenzoxazine, as proposed for resorcinol-formaldehyde polymer by Nishiyama et al. [45]. The cationic head group of CTAB molecules was interacted with the anionic OH^- group of polybenzoxazine chain, leading to an enlargement of polybenzoxazine chain spacing by CTAB molecules [45], resulting in slightly change in an average mesopore diameter from 34.78 nm to 35.85 and 36.07 nm for CX, CX-CTAB-0.003, and CX-CTAB-0.009, respectively. However, at the CTAB concentrations of 0.030, 0.090, and 0.180 M, carbon xerogels nanospheres were obtained by the formation of benzoxazine clusters inside the interior region of CTAB micelles, not resulted from the phase separation phenomena. Therefore, in this case, mesopore structures were mainly affected by the size of benzoxazine nanospheres generated inside the inner core of CTAB micelles. After the benzoxazine nanospheres grew inside the interior region of micelles, the inter-connection between benzoxazine nanospheres could be taken place due to the ring opening polymerization of oxazine rings at the surface of each nanopsheres, as proposed for resorcinol-formaldehyde polymer by Lee et al. [22], leading to inter-connected structure of nanospheres with smaller mesopore and more dense morphologies comparing to those of CX, CX-CTAB-0.003, and CX-CTAB-0.009.

Figure 5.3 presents the nitrogen adsorption-desorption isotherm of all samples. According to classification by IUPAC, all samples show the standard isotherm of type IV representing the characteristics of mesoporous adsorbent. However, the hysteresis loop obtained from reference carbon (CX) and carbon xerogels with low concentration of CTAB (0.003 and 0.009 M) are of H3 in which the hysteresis loop H3 representing the aggregation of platy particles or adsorbents containing slit-shape pores [21, 47]. As the concentrations of CTAB were increased to 0.030-0.180 M, the carbon xerogels exhibited the hysteresis loop of H1 representing the narrow distribution of uniform pore [47]. Moreover, all samples show the amount of uptake at relative pressure of 0.75-1.00 implying the adsorption

of large mesopore diameter, as shown in Table 5.2. CX-CTAB-0.090 shows the highest amount of uptake indicating a high porosity compared to other samples.

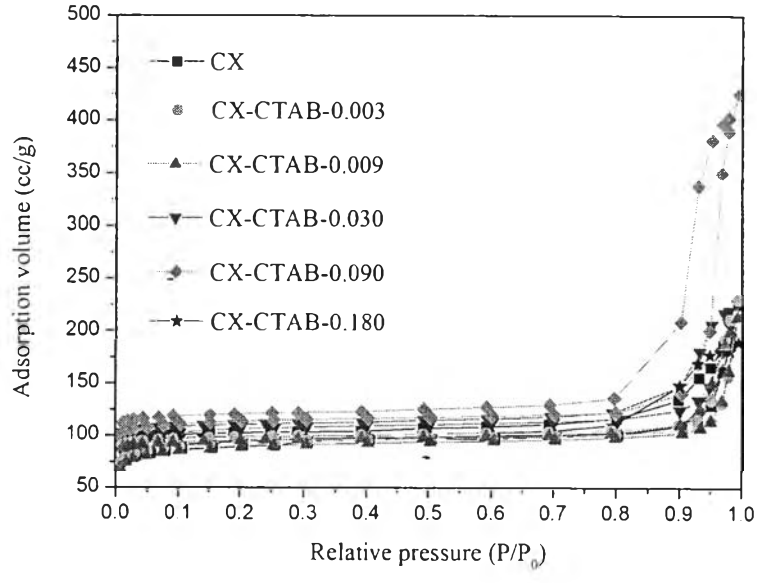

Figure 5.3 N_2 adsorption-desorption isotherms of polybenzoxazine-based carbon xerogels using different concentrations of CTAB.

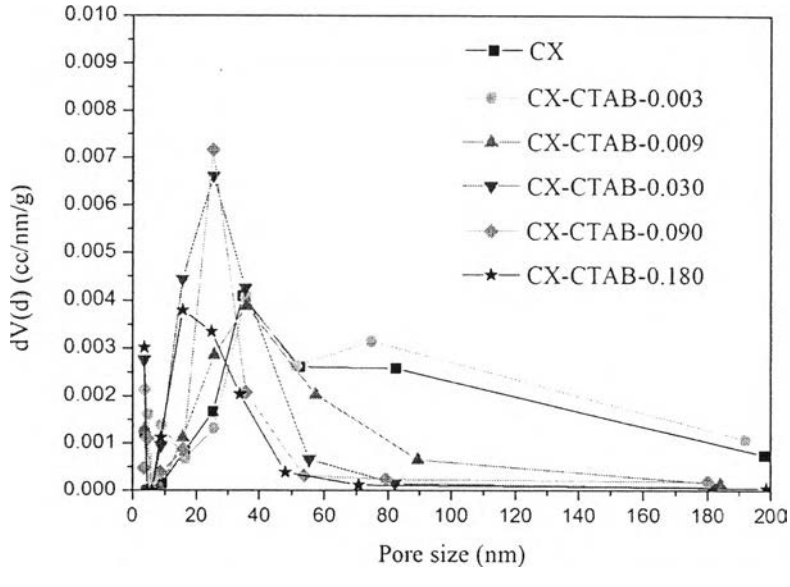

Figure 5.4 Mesopore size distributions of polybenzoxazine-based carbon xerogels using different concentrations of CTAB, determined by BJH method.

The pore size distribution of all samples, calculated by BJH method, was illustrated in Figure 5.4. All samples show an average mesopore size ranging from 15.57-36.07 nm and an average mesopore size was also decreased when the inter-connection of carbon xerogel nanospheres were formed. Carbon xerogels with high concentration of CTAB (0.030 M, 0.090 M, and 0.180 M) mainly exhibit the narrower pore size distribution in the range of 5-50 nm comparing to those of reference carbon xerogels and carbon xerogels with low concentration of CTAB (ranging 5-85 nm) corresponding to the hysteresis loop of H1 indicating the narrow distribution of uniform pores [47].

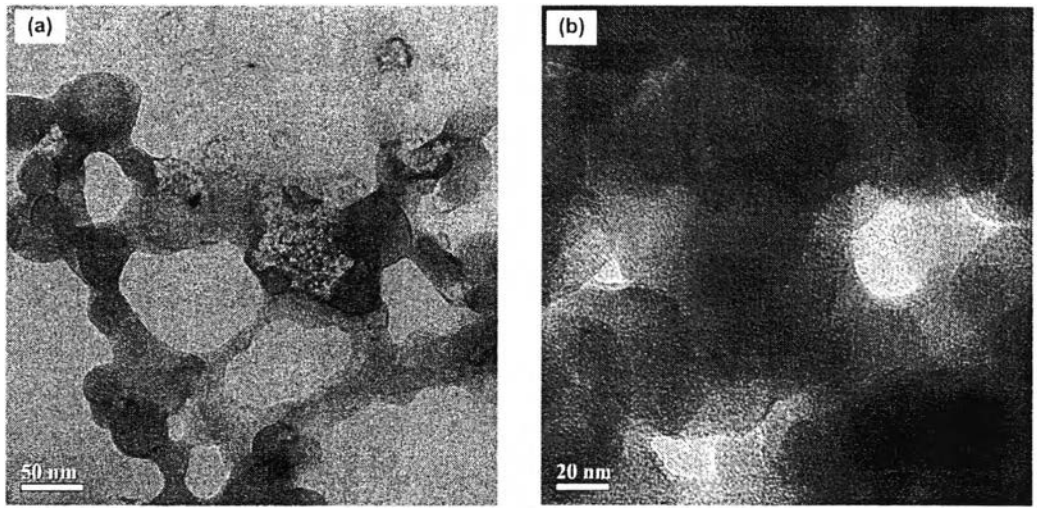

Figure 5.5 TEM images of PBZ-based carbon xerogels prepared from 10% w/w of benzoxazine precursor using 0.090 molar of CTAB; (a) low magnification, (b) high magnification.

TEM images of CX-CTAB-0.090 are illustrated in Figure 5.5 indicating the pores inside the samples were created by the inter-connected structure of carbon particles similar to those proposed by Lee et al. [22]. Moreover, the particle sizes obtained from TEM technique were also corresponded to those obtained from FE-SEM technique in which the particle sizes generated by CTAB micelles were about 50-100 nm in size.

5.4.2 Effects of Non-ionic surfactant (Polyethylene glycol nonylphenyl-ether, Synperonic NP30) on porous structure of PBZ-based carbon xerogels

Polybenzoxazine (PBZ)-based carbon xerogels were synthesized by using Synperonic NP30 as a non-ionic surfactant as described in experimental section. The morphologies of the obtained PBZ-based carbon xerogels were observed by FE-SEM technique. Figure 5.6 shows the SEM micrographs of PBZ-based carbon xerogels synthesized at different concentrations of Synperonic NP30 from 0.003 M to 0.180 M. All samples, except CX-NP30-0.180, show the inter-connected network formed by aggregated-fused carbon nanoparticles. Furthermore, CX-NP30-0.180 (Figure 5.6f) shows the inter-connected structure with opened network and loose structure, formed by 2.5 μm of carbon xerogel microspheres. As the concentrations of Synperonic NP30 were increased from 0.003 M to 0.090 M, the networks of the obtained carbon xerogels became less packed and the open network in the range of micrometer scale were achieved. Figures 5.6c-f show the open network structures in the range of micrometer scale with very loose network packing, especially, at 0.090 and 0.180 M. Moreover, at the concentration of 0.180 M, the carbon xerogel microspheres of 2.5 μm were obviously obtained.

To explain the formation of carbon xerogel microspheres, the micelle formation of Synperonic NP30 was used to explain, like those mentioned in the case of CTAB (section 3.1). If the concentration of Synperonic NP30 was equal to the critical micelle concentration (CMC), the molecules of Synperonic NP30 was then oriented as spherical shape with hydrophilic head groups at exterior region and hydrophobic tail groups at interior region of the micelles. Polybenzoxazine cluster would be then formed at the interior region of the micelle and then grow into microspherical shape. After that, the interconnection between benzoxazine microspheres could be taken place due to the ring opening polymerization of oxazine rings at the surface of each microsphere as described in section 3.1 of the CTAB system [22]. Figure 5.2b illustrates the formation model of polybenzoxazine xerogel microspheres formed inside the interior region of Synperonic NP30 micelles. In

2011, Wang et al. found that carbon aerogel microspheres could be produced by using non-ionic surfactant, called SPAN 80, in the range of 2-50 μm in sizes [48]. As mention above, CX-NP30-0.180 was the carbon xerogel microspheres implying that the Synperonic NP30 molecules start to form spherical micelles at 0.180 M. Although the carbon xerogel microspheres were spherical like those derived from the CTAB system, the carbon xerogel microspheres obtained from Synperonic NP30 system were also bigger. The reason for this phenomenon can be described by the formation of bigger micelles of Synperonic NP30 molecules comparing to those of CTAB molecules, as proposed in Figure 5.2.

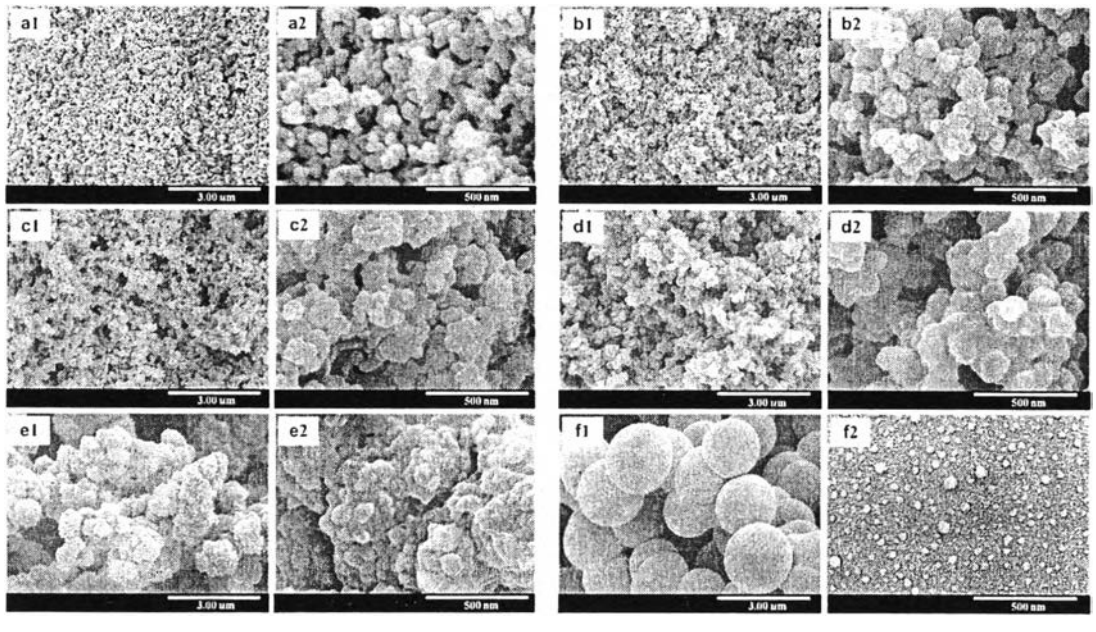

Figure 5.6 SEM micrographs of PBZ-based carbon xerogels prepared from 10% w/w of benzoxazine precursor using different concentrations of Synperonic NP30; (a) no added CTAB, (b) 0.003 M, (c) 0.009 M, (d) 0.030 M, (e) 0.090 M, and (f) 0.180 M; 1: low magnification; 2: high magnification.

The porous structures of PBZ-based carbon xerogels using Synperonic NP30 as a surfactant were tabulated in Table 5.2. All samples show the comparative BET surface area about 262-290 m^2/g. Higher amount of mesopore volume comparing to micropore volume was obtained, about 0.20 cc/g for reference carbon xerogel (CX) and 0.34 cc/g for CX-NP30-0.003. However, when the concentration of Synperonic NP30 was changed from 0.009 M to 0.090 M, the samples showed higher amount of micropore volume, about 0.13 cc/g comparing to amount of mesopore volume. Moreover, after the concentration of Synperonic NP30 reached 0.180 M, CX-NP30-0.180 was almost dominated by micropore volume in the structure, about 0.12 cc/g comparing to mesopore volume of 0.04 cc/g. Pointing to an average mesopore diameter of all samples, we found that an average mesopore diameter was increased from 34.78 nm for reference carbon xerogel (CX) to 56.78 nm for low concentration of Synperonic NP30 (0.003 M). Hence, the large mesopore obtained from CX and CX-NP30-0.003 should be generated by the inter-connected structure of carbon xerogel particles like those proposed by Wang et al. [16]. The expansion of mesopore diameter from 34.78 nm for CX to 56.78 nm for CX-NP30-0.003 could be explained by the enlargement of benzoxazine chain spacing resulted from the Synperonic NP30 molecules, as mentioned in section 3.1 and proposed by Nishiyama et al. [45]. Then, increasing concentrations of Synperonic NP30, mesopores diameter were also decreased into small mesopore diameter in the range of 3.57-6.20 nm for the concentrations of 0.009-0.180 M (CX-NP30-0.009 to CX-NP30-0.180). Furthermore, when the concentration was increased from 0.009 M to 0.180 M, the large opened network and the loose structure in the range of micrometer scale were obviously observed by FE-SEM technique as well (Figures 5.6c-f). However, the large opened network could not be detected by N_2 adsorption technique due to the limitation of Kelvin equation [3]. According to the model proposed by Wang et al. [16], the micropore (2 nm $\leq$) and small mesopore (2-5 nm) were located within the carbon nanoparticles. Therefore, from the results, the obtained small mesopore in the range of 3.57-6.20 nm (for CX-NP30-0.009 to CX-NP30-0.180) should be more likely to be located in the carbon xerogel particles rather than generated by the inter-connected structure of carbon particles like CX and CX-NP30-

0.003. Moreover, an average micropore diameter of all samples was in the range of 0.66-1.00 nm.

Table 5.2 Pore structure of PBZ-based carbon xerogels prepared from 10% w/w of benzoxazine precursor using different concentrations of Synperonic NP30

Sample	S_{BET} (m^2/g)	V_{micro} (cm^3/g)	V_{meso} (cm^3/g)	V_{total} (cm^3/g)	APD_{micro} (nm)	APD_{meso} (nm)
CX	280	0.08	0.20	0.28	0.76	34.78
CX-NP30-0.003	284	0.08	0.34	0.42	0.66	56.78
CX-NP30-0.009	276	0.13	0.08	0.21	0.70	6.20
CX-NP30-0.030	290	0.13	0.09	0.22	0.66	3.57
CX-NP30-0.090	292	0.13	0.08	0.21	0.76	3.57
CX-NP30-0.180	262	0.12	0.04	0.16	1.00	4.53

Notes : S_{BET}: BET surface area; S_{meso}: mesopore surface area; V_{micro}: micropore volume; V_{meso}: mesopore volume; V_{total}: total pore volume; APD_{micro}: average micropore diameter; APD_{meso}: average mesopore diameter; APD: average pore diameter

Figure 5.7 illustrates the nitrogen adsorption-desorption isotherm of all samples. According to classification by IUPAC, CX and CX-NP30-0.003 exhibited the standard isotherm of type IV with H3 hysteresis loop. Type IV represents the characteristics of mesoporous material and H3 represents the aggregation of platy particles or adsorbents containing slit-shape pores [21, 47]. However, as the concentration of Synperonic NP30 was increased from 0.009 to 0.180 M, all samples exhibited the standard isotherm of type Ia representing microporous absorbents with pores of molecular dimensions (very small micropore) [47].

The mesopore size distribution of all samples, calculated by BJH method, was illustrated in Figure 5.8. CX and CX-NP30-0.003 show higher amount of mesopore volume and lager average mesopore size about 0.20-0.34 cc/g and 34.78-56.78 nm, respectively, than those of other samples. An average mesopore size was also shifted to smaller mesopore diameters ranging from 3.57 nm to 6.20 nm, when increasing the concentration of Synperonic NP 30. Moreover, from Figure 5.8,

amount of mesopore volume of carbon xerogels derived from Synperonic NP30 at concentration of 0.009-0.180 M, was clearly lower than those of CX and CX-NP30-0.003 as well.

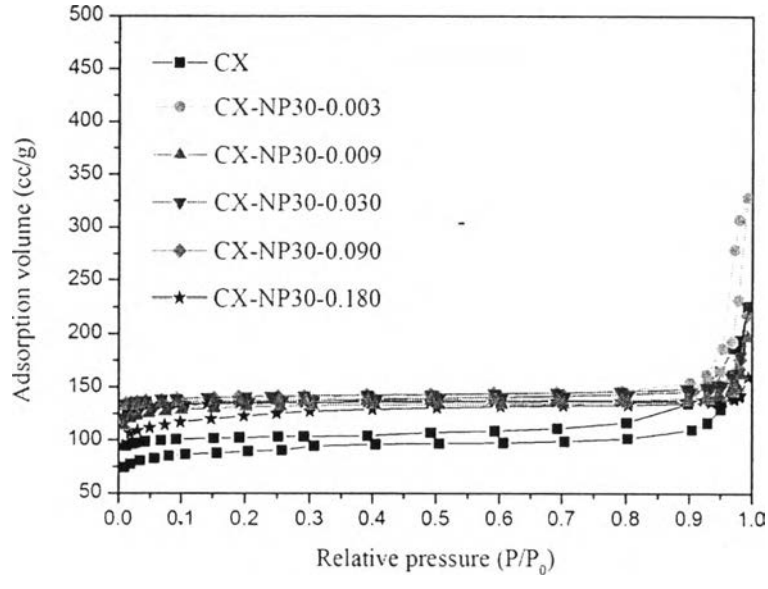

Figure 5.7 N_2 adsorption-desorption isotherms of polybenzoxazine-based carbon xerogels using different concentrations of Synperonic NP30.

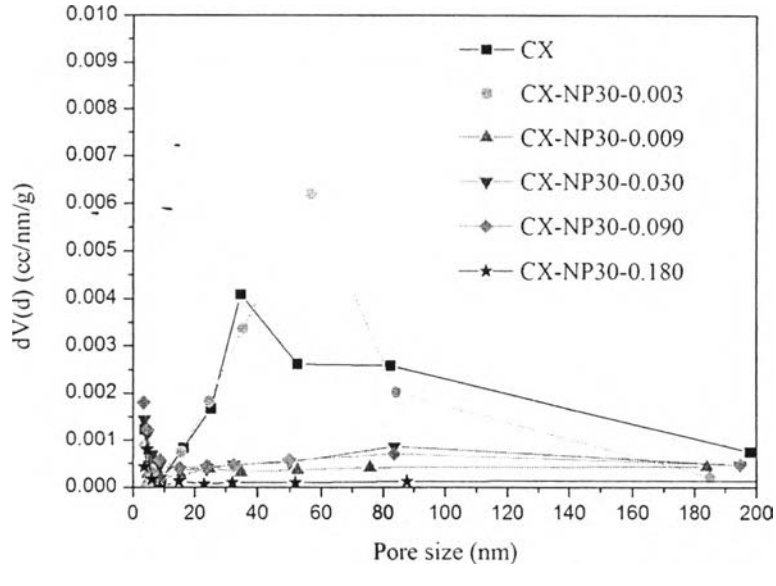

Figure 5.8 Mesopore size distributions of polybenzoxazine-based carbon xerogels using different concentrations of Synperonic NP30, determined by BJH method.

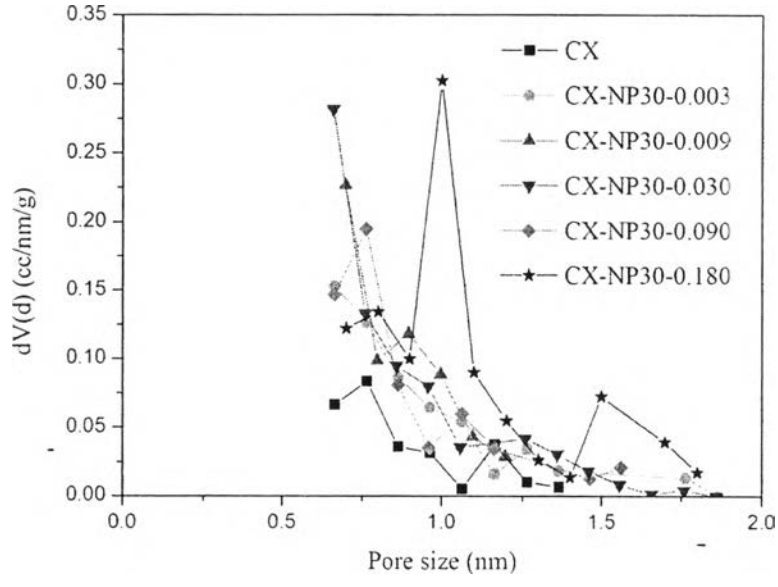

Figure 5.9 Micropore size distributions of polybenzoxazine-based carbon xerogels using different concentrations of Synperonic NP30, determined by MP method.

According to the microporous property of the obtained carbon xerogels, micropore size distributions, calculated by MP method (standard micropore size distribution), were shown in Figure 5.9. All samples showed the micropore size distribution in the range of very small micropores of 0.66-1.00 nm corresponding to the standard isotherm of type Ia representing the microporous absorbent with pore of molecular dimensions (very small micropore) [47]. Moreover, when the concentration of Synperonic NP30 were in the range of 0.009-0.180, as shown in Figure 5.9, the obtained carbon xerogels clearly showed high amount of micropore volume comparing to those of CX and CX-NP30-0.003.

5.5 Conclusions

By using non-ionic surfactant (Synperonic NP30) and cationic surfactant (CTAB), the carbon xerogels derived from polybenzoxazine with tunable pore structure were successfully synthesized by a facile synthesis process with shorter preparation time. When CTAB was used as a surfactant, mesoporous carbon xerogels with wide range of mesopore diameters were obtained by changing the

concentrations of CTAB. The mesopore diameters of 35.85, 36.07, 25.38, 25.25, and 15.57 nm were achieved for CTAB concentration of 0.003, 0.009, 0.030, 0.090, and 0.180 M, respectively. Carbon xerogel with the CTAB concentration of 0.090 M (CX-CTAB-0090) showed the highest mesoporosity of 0.64 cc/g and the highest BET surface area of 369 m^2/g. Moreover, the carbon xerogel nanospheres with the size of 50-200 nm were obtained through emulsion process since the concentration of CTAB was equal to or exceeded 0.030 M. On the other hand, when the Synperonic NP30 concentrations were increased, the properties of the obtained carbon xerogels were shifted from mesoporous material for reference carbon xerogel (CX) to obviously microporous material at higher concentrations of Synperonic NP30 (0.009-0.180 M). Furthermore, the carbon xerogel microspheres with size of about 2.5 μm were obtained through the emulsion process when the concentration of Synperonic NP30 reached 0.180 M. Therefore, CTAB is a suitable surfactant to produce mesoporous carbon xerogels with wide ranges of large mesopore diameters through the emulsion process and Synperonic NP30 is suitable for producing the microporous carbon xerogels, especially, microporous microspheres. Hence, the porous structure of polybenzoxazine-based carbon xerogels could be easily tailored by changing the surfactant species and concentrations.

5.6 Acknowledgements

This work has been financially supported by the Petroleum and Petrochemical College and the Center of Excellence on Petrochemical and Materials Technology, Chulalongkorn University. In addition, the authors would like to thank Mr. Tony Bennett for proof-reading this manuscript. The authors also would like to express their deep appreciation to the Office of Higher Education Commission (OHEC), Thailand, for its financial support on this project under Climate Change cluster (CC557A) of the National Research University Program.

5.7 References

[1] R.W. Pekala, Organic aerogels from the polycondensation of resorcinol with formaldehyde, J. Mater. Sci. 24 (1989) 3221-3227.

[2] R.W. Pekala, D.W. Schaefer, Structure of organic aerogels. 1. Morphology and scaling, Macromolecules 26 (1993) 5487-5493.

[3] N. Job, A. Thery, R. Pirard, J. Marien, L. Kocon, J.N. Rouzaud, F. Beguin, J.P Pirard, Carbon aerogels, cryogels and xerogels: Influence of drying method on textural properties of porous carbon materials, Carbon 43 (2005) 2481-2494.

[4] H. Tamon, H. Ishizaka, T. Yamamoto, T. Suzuki, Preparation of mesoporous carbon by freeze drying, Carbon 37 (1999) 2049-2055.

[5] C. Arbizzani, S. Beninati, E. Manferrari, F. Soavi, M. Mastragostino, Cryo- and xerogel carbon supported PtRu for DMFC anodes, J. Power Sources 172 (2007) 578-586.

[6] C.S. Sharma, M.M. Kulkarni, A. Sharma, M. Madou, Synthesis of carbon xerogel particles and fractal-like structures, Chem. Eng. Sci. 64 (2009) 1536-1543.

[7] J. Shen, J. Hou, Y. Guo, H. Xue, G. Wu, B. Zhou, Microstructure control of RF and carbon aerogels prepared by sol-gel process, J. Sol-Gel Sci. Technol. 36 (2005) 131-136.

[8] E. Antolini, Carbon supports for low-temperature fuel cell catalyst, Appl. Catal., B 88 (2009) 1-24.

[9] C. Moreno-Castilla, F.J. Maldonado-Hodar, Carbon aerogel for catalysis applications: An overview, Carbon 43 (2005) 455-465.

[10] H. Kabbour, T.F. Baumann, J.H. Satcher Jr., A. Saulnier, C.C. Ahn, Toward new candidates for hydrogen storage: High-surface-area carbon aerogels, Chem. Mater. 18 (2006) 6085-6087.

[11] S. Sepehri, B.B. Garcia, Q. Zhang, G. Cao, Enhanced electrochemical and structural properties of carbon cryogels by surface chemistry alteration with boron and nitrogen, Carbon 47 (2009) 1436-1443.

[12] R.W. Pekala, J.C. Farmer, C.T. Alviso, T.D. Tran, S.T. Mayer, J.M. Miller, B. Dunn, Carbon aerogels for electrochemical applications, J. Non-Cryst. Solids 225 (1998) 74-80.

[13] A.F. Ismail, L.I.B. David, A review on the latest development of carbon membranes for gas separation, J. Membr. Sci. 193 (2001) 1-18.

[14] C.W. Jones, W.J. Koros, Carbon molecular sieve gas separation membranes-I.Preparation and characterization based on polyimide precursors, Carbon 32 (1994) 1419-1425.

[15] V. Bock, A. Emmerling, R. Saliger, J. Fricke, Structural investigation of resorcinol formaldehyde and carbon aerogels using SAXS and BET, J. Porous Mater. 4 (1997) 287-294.

[16] J. Wang, X. Yang, D. Wu, R. Fu, M.S. Dresselhaus, G. Dresselhaus, The porous structures of activated carbon aerogels and their effects on electrochemical performance, J. Power Sources 185 (2008) 589-594.

[17] Y. Hanzawa, H. Hatori, N. Yoshizawa, Y. Yamada, Structural changes in carbon aerogels with high temperature treatment, Carbon 40 (2002) 575-581.

[18] Y. Hanzawa, K. Kaneko, R.W. Pekala, M.S. Dresselhaus, Activated carbon aerogels, Langmuir 12 (1996) 6167-6169.

[19] A.M. Puziy, O.I. Poddubnaya, A. Martinez-Alonso, F. Suarez-Garcia, J.M.D. Tascon, Synthetic carbons activated with phosphoric acid: II.Porous structure, Carbon 40 (2002) 1507-1519.

[20] M. Liu, L. Gan, C. Tian, J. Zhu, Z. Xu, Z. Hao, L. Chen, Mesoporous carbon foams through surfactant templating, Carbon 45 (2007) 3045-3046.

[21] I. Matos, S. Fernandes, L. Guerreiro, S. Barata, A.M. Ramos, J. Vital, I.M. Fonseca, The effect of surfactants on the porosity of carbon xerogels, Micrōpor. Mesopor. Mater. 92 (2006) 38-46.

[22] K.T. Lee, S.M. Oh, Novel synthesis of porous carbons with tunable pore size by surfactant-templated sol-gel process and carbonization, Chem. Commun. 22 (2002) 2722-2723.

[23] D. Wu, R. Fu, M.S. Dresselhaus, G. Dresselhaus, Fabrication and nano-structure control of carbon aerogels via a microemulsion-templated sol-gel polymerization method, Carbon 44 (2006) 675-681.

[24] J. Gorka, M. Jaroniec, Hierarchically porous phenolic resin-based carbons obtained by block copolymer-colloidal silica templating and post-synthesis activation with carbon dioxide and water vapor, Carbon 49 (2011) 154-160.

[25] T.F. Baumann, J.H. Satcher Jr., Template-directed synthesis of periodic macroporous organic and carbon aerogels, J. Non –Cryst. Solids 350 (2004) 120-125.
[26] D. Wu, R. Fu, S. Zhang, M.S. Dresselhaus, G. Dresselhaus, Preparation of low-density carbon aerogels by ambient pressure drying, Carbon 42 (2004) 2033-2039.
[27] Y. Zhu, H. Hu, W. Li, H. Zhao, Preparation of cresol–formaldehyde carbon aerogels via drying aquagel at ambient pressure, J. Non-Cryst. Solids 352 (2006) 3358-3362.
[28] R.W. Pekala, C.T. Alviso, X. Lu, J. Gross, J. Fricke, New organic aerogels based upon a phenolic-furfural reaction, J. Non-Cryst. Solids 188 (1995) 34-40.
[29] H. Tamon, H. Ishizaka, M. Mikami, M. Okazaki, Porous structure of organic and carbon aerogels synthesized by sol-gel polycondensation of resorcinol with formaldehyde, Carbon 35 (1997) 791-796.
[30] X. Ning, H. Ishida, Phenolic materials via ring-opening polymerization: Synthesis and characterization of bisphenol-A based benzoxazines and their polymer, J. Polym. Sci., Part A: Polym. Chem. 32 (1994) 1121-1129.
[31] N.N. Ghosh, B. Kiskan, Y. Yagci, Polybenzoxazines-New high performance thermosetting resins: Synthesis and properties, Prog. Polym. Sci. 32 (2007) 1344-1391.
[32] T. Agag, T. Takeichi, High-molecular-weight AB type benzoxazines as new precursors for high performance thermosets, J. Polym. Sci., Part A: Polym. Chem. 45 (2007) 1878-1888.
[33] T. Takeichi, T. Kano, T. Agag, Synthesis and thermal cure of high molecular weight polybenzoxazine precursors and the properties of the thermosets, Polymer 46 (2005) 12172-12180.
[34] Z. Brunovska, J.P. Liu, H. Ishida, 1,3,5-Triphenylhexahydro-1,3,5-triazine – active intermediate and precursor in the novel synthesis of benzoxazine monomers and oligomers, Macromol. Chem. Phys. 200 (1999) 1745-1752.
[35] P. Lorjai, T. Chaisuwan, S. Wongkasemjit, Porous structure of benzoxazine-based organic aerogel prepared by sol-gel process and their carbon aerogels, J. Sol-Gel Sci. Technol. 52 (2009) 56-64.

[36] P. Katanyoota, T. Chaisuwan, A. Wongchaisuwat, S. Wongkasemjit, Novel polybenzoxazine-based carbon aerogel electrode for supercapacitors, Mater. Sci. Eng., B 167 (2010) 36-42.

[37] J. Perez-Ramirez, F. Kapteijn, J.C. Groen, A. Domenech, G. Mul, J.A. Moulijn, Steam-activated FeMFI zeolites. Evolution of iron species and activity in direct N_2O decomposition, J. Catal. 214 (2003) 33-45.

[38] S. Donk van, A. Broersma, O.L.J. Gijzeman, J.A. Bokhoven van, J.H. Bitter, K.P. Jong de, Combined Diffusion, Adsorption, and Reaction Studies of *n*-Hexane Hydroisomerization over Pt/H–Mordenite in an Oscillating Microbalance, J. Catal. 204 (2001) 272-280.

[39] H. Ishida, Process for preparation of benzoxazine compounds in solventless systems, US Pat. 5 543 516 1996.

[40] U. Thubsuang, H. Ishida, S. Wongkasemjit, T. Chaisuwan, Novel template confinement derived from polybenzoxazine-based carbon xerogels for synthesis of ZSM-5 nanoparticles via microwave irradiation, Micropor. Mesopor. Mater. 156 (2012) 7-15.

[41] S. Brunauer, P.H. Emmett, E. Teller. Adsorption of gases in multimolecular layers, J. Am. Chem. Soc. 60 (1938) 309–319.

[42] B.C. Lippens, J.H. Boer de, Studies on pore systems in catalysts: V. The *t* method, J. Catal. 4 (1965) 319-323.

[43] E.P. Barrett, L.G. Joyner, P.P. Halenda, The determination of pore volume and area distributions in porous substances. I. Computations from nitrogen isotherms, J. Am. Chem. Soc. 73 (1951) 373–380.

[44] L.G. Joyner, E.P. Barrett, R. Skold, The determination of pore volume and area distributions in porous substances. II. Comparison between nitrogen isotherm and mercury porosimeter methods, J. Am. Chem. Soc. 73 (1951) 3155–3158.

[45] N. Nishiyama, T. Zheng, Y. Yamane, Y. Egashira, K. Ueyama, Microporous carbons prepared from cationic surfactant-resorcinol/formaldehyde composites, Carbon 43 (2005) 269-274.

[46] M.J. Rosen, Surfactant and interfacial phenomena, third ed., John Wiley & Sons, Inc., Hoboken, New Jersey, 2004.

[47] F. Rouquerol, J. Rouquerol, K.S.W. Sing, Adsorption by Powders and Porous

Solids, Principles, Methodology and Applications, Academic press, London, 1999.
[48] X. Wang, X. Wang, L. Liu, L. Bai, H. An, L. Zheng, L. Yi, Preparation and characterization of carbon aerogel microspheres by an inverse emulsion polymerization. J. Non –Cryst. Solids 357 (2011) 793-797.